CHARACTERIZATION OF A BLURRY INJECTOR FOR BIOFUELS

Claudia Gonçalves de Azevedo, claudia@lcp.inpe.br
Fernando de Souza Costa, fernando@lcp.inpe.br
National Institute for Space Research, Associated Laboratory of Combustion and Propulsion, Rodovia Presidente Dutra, km 40, Cachoeira Paulista, SP, 12630-000, Brazil

Heraldo da Silva Couto, heraldo.couto@vsesa.com.br
Vale Energy Solution, Rodovia Presidente Dutra, km 138, São José dos Campos, SP, 12247-004, Brazil

Abstract. *The increase of oil prices, the growing environmental concerns, and more stringent regulations on fuel emissions have caused a significant interest on biofuels, especially ethanol and biodiesel. In general, liquid fuels are atomized to yield a larger liquid surface area, therefore providing larger vaporization and mixing rates. A blurry injector is an air-blast injector that presents a backflow of gas into the liquid feed tube. It can generate a relatively uniform spray with small droplets. This paper describes the injection characteristics of water, hydrous ethanol and B100 soy biodiesel through a blurry injector. Average diameters, mass flow rates, discharge coefficients and spray cone angles for different injection pressures and air-liquid ratios are presented.*

Keywords*: Blurry injector, Biofuels, Laser diffraction technique*

1. INTRODUCTION

In recent years there has been a great interest in the use of biofuels in order to reduce the environmental impact of combustion processes and replacement of fossil fuels. Therefore, it is of interest to the country and companies to investigate the use of this biofuels in industrial applications, aiming to reduce costs, increase operating efficiency and reduce pollutants emissions. Nowadays, the most commonly used alternative fuels in the world are biodiesel and ethanol.

The atomization of a liquid into small droplets in the form of a spray is an important process in industrial, combustion and propulsion system. A larger surface area is produced by forming droplets, thus reducing the liquid vaporization time. In liquid fuel combustion application this results in better mixing and an increase in the time available for complete combustion (Lefebvre, 1983).

The process of atomization is a physical process in which a jet, sheet or a film of liquid is disintegrated by the kinetic energy of the liquid itself, by exposure to a stream of air or gas of high speed, or as a result of external mechanical energy (Lefebvre, 1989). In the atomization process a volume of fuel is converted into a multiplicity of small droplets, aiming to increase the contact area between the fuel and oxidizer and, therefore, to increase the rates of mixing and fuel evaporation.

Based on a flow-focusing injector, Gañan-Calvo (2005) describes the flow-blurring injector, or blurry injector, which presents several advantages over other injectors, such as formation of a uniform spray, better atomization, high atomization efficiency, robustness, excellent fuel vaporization and mixture with air, and potential for application in compact combustion systems which can be used as portable power sources. According to Gañan-Calvo (2005), for given values of liquid flow and total energy input, the flow blurring configuration is capable of creating about 5 and 50 times more droplet surface area than other pneumatic nebulizers. Figure 1 shows a scheme of the flow-blurring injector.

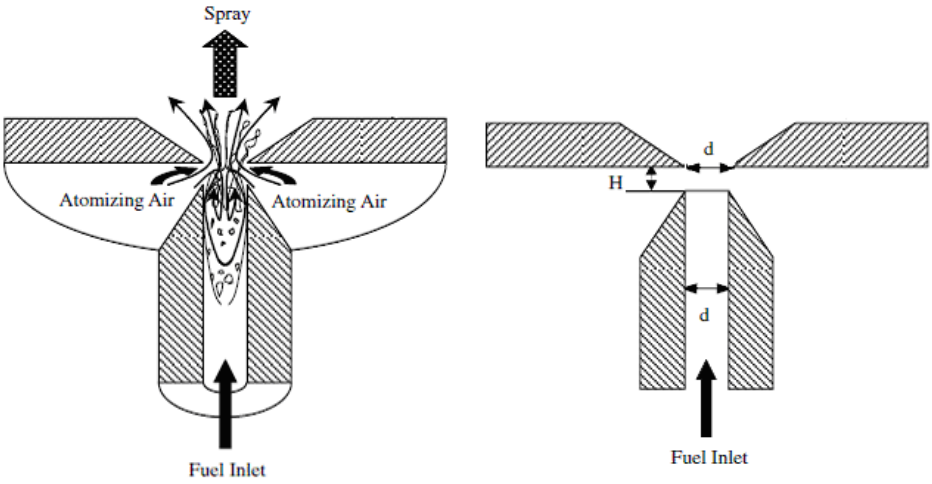

Figure 1. Schematic the Flow-Blurring Injector: flow structure and geometric details.

The liquid to be atomized exits from a feed tube whose inner diameter is equal to the exit orifice diameter *d*, located in the orifice plate, as seen in Fig. 1. Both sections are perfectly aligned and separated by a distance *H*. Thus, the gap between the feed tube end and the exit orifice gives rise to a lateral cylindrical passageway, LCP. It is worth noting that the LCP surface equals the exit orifice area when $c = H/D = 0.25$. Consequently, when a liquid mass flow rate $\dot{m}_l$ is forced through the feed tube and a gas mass flow rate $\dot{m}_g$ is forced through the LCP, a spray combining both phases is formed and leaves the device through the orifice exit.

The flow-blurring mechanism is characterized by a global bifurcation of liquid-gas flow at the tip of the feed tube of liquid. This bifurcation is triggered by a single fundamental geometrical parameter $c = H/D$. When *c* is decreased to about 0.25 a radical modification in the flow configuration is observed. The gas accelerates radially towards the liquid exiting the feed tube and there is a return of the gas flow into the feeding tube of the liquid (backflow), creating a recirculation flow within the tube, that results in a turbulent interaction between the phases and thus creating a spray of small droplets. The backflow pattern produces efficient mixing between the gas and liquid phases, and leads to energy-efficiency improvements over other atomization process.

Panchasara *et al.* (2009) compared experimentally a flow blurring injector with a commercial air-blast injector, using kerosene and diesel burning in air at ambient pressure, and verified that the flow blurring injector produced 3 to 5 times lower NO_x and CO emissions as compared to the air-blast injector. Sadasivuni and Agrawal (2009) used the flow blurring injector in a compact combustion system with a counter flow heat exchanger. The volumetric energy density of the system was substantially higher than that of the concepts developed previously. Heat release rate of up to 460 W was achieved in a combustor volume of 2.0 cm^3. The combustion system produced clean, compact, quiet, distributed, attached flat flame. No soot or coking problems were experienced during or after combustor operation on kerosene fuel. Simmons and Agrawal (2010) used laser sheet visualization and a phase Doppler particle analyzer to obtain the spray characteristics of a flow blurring injector operating with a configuration where $H/D = 0.23$ and using as working fluids water and air. The authors compared performance of the above injector with that of an air-blast injector and from the results concluded that the flow blurring injector can effectively atomize liquids at relatively low air-to-liquid mass ratio compared to the air-blast injector, while reducing the pressure drop penalty in the atomizing air line.

Therefore, this work aims to present the characterization of a blurry injector for injection of water, hydrous ethanol and B100 soy biodiesel. Experiments are conducted for different atomizing air-to-liquid mass ratios (ALRs) and injection pressures.

2. EXPERIMENTAL SECTION

Figure 2 shows a schematic for a blurry injector.

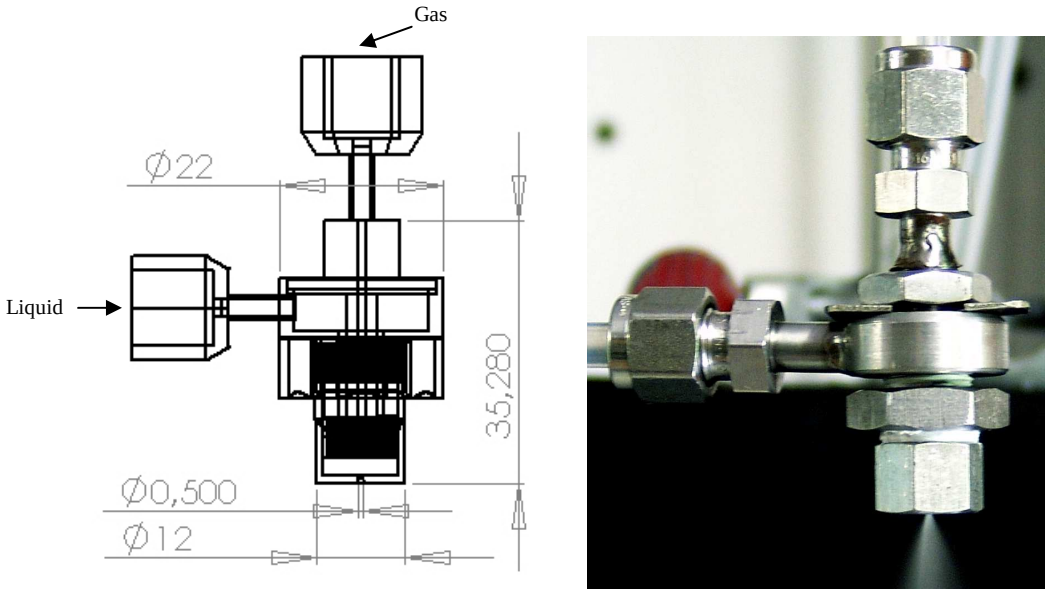

Figure 2. Schematic representation and photos of the Blurry injector.

The injector is composed by a liquid feed tube ($d = 0.5$ mm), a coannular atomizing air passage and an orifice plate, whose exit orifice diameter is equal to diameter of feed tube *d*. The two-phase mixture exits through the exit orifice in the orifice plate located at a distance *H* ranging from 0.075 a 0.125 mm. The air is supplied to the air chamber that

ascertains the uniform distribution of air through the coannular atomizing air passage. The efficient mixing between the air and liquid phases produces a fine spray.

Spray characteristics are generally measured by considering the macroscopic and microscopic structure of the spray. The macroscopic structure of the spray, such as cone angle, is measured conventionally by high-speed photography, and the microscopic structure of the spray, such as the droplet size distribution, can be measured by laser-based techniques.

2.1. Droplet size measurement

The laser diffraction method was used to measure the Sauter mean diameter (SMD), which is defined as the diameter of a drop having the same volume/surface ratio as the entire spray, i.e.,

$$D_{32} = \frac{\sum_{i=1}^{n} d_i^3}{\sum_{i=1}^{n} d_i^2} \tag{1}$$

Figure 3 shows the drop size measurement system used in this study. The Malvern Spraytec® system was used to measure the drop size distribution. The instrument measures the variation in angular scattering as a function of particle size for a group of particles.

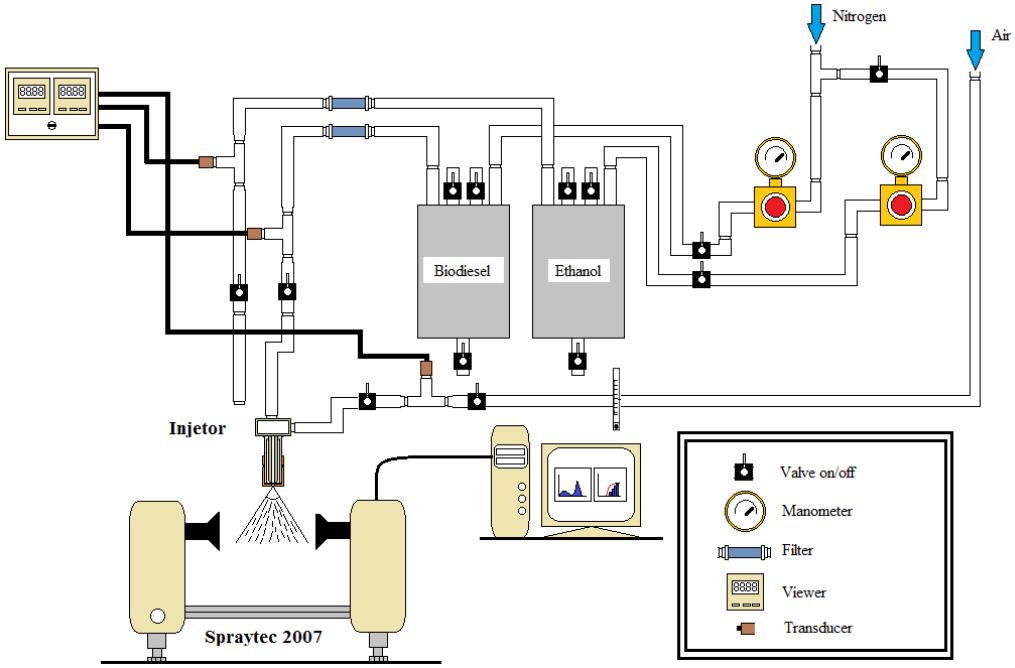

Figure 3. Schematic representation of the test bench.

The Spraytec® takes into account multiple light scattering and contains two major differences compared with the previous versions: first, the system employs the Lorenz-Mie theory to take into account the contribution of the angular light energy distribution of refraction through small droplets, which considerably improves a behavior of the instrument when measuring very fine sprays, and second, the mathematical inversion procedure of the system includes a patented multiple-scattering algorithm that allows successful measurements in extremely high concentrations with light obscuration as high as 95% (5% transmission).

Laser measurements were taken 50 mm downstream of the exit of the injector, where the spray drop size was constant further downstream. The centre of the spray was positioned at the laser beam centre, so the spray could be fully covered by the laser beam. The values of MMD (mass median diameter) and SMD (Sauter mean diameter) were obtained by averaging three runs.

The working fluids used in the present study were water and ethanol at room temperature, which were supplied to the atomizer from the liquid inlet port of 0.5 mm in diameter. The properties of the liquids in this study are shown in Tab. 1 at laboratory ambient conditions of 298.15-301.15 K and 95 kPa. Density ρ, surface tension σ, and dynamic viscosity μ were determined by measurement in laboratory.

Table 1. Properties liquid fuels at 95 kPa.

Liquid	Surface Tension σ (N/m)	Density ρ (kg/m^3)	Dynamic Viscosity μ (Ns/m^2)
Water	0.072 (2)	996.66 (3)	0.0008325 (3)
Hydrous ethanol	0.024 (2)	806.7 (1)	0.00124 (3)
B100 soy biodiesel	0.028 (3)	875.7 (3)	0.0048 (3)

(1): measured at 25°C (2): measured at 26°C (3): measured at 28°C

2.2 Spray cone angle

Another important parameter in characterization of the injector is the spray cone angle, which can influence directly the combustion and the flame length. Generally, the spray formed in the process of atomization has initially the shape of a cone. The opening angle is related to the penetration capability of the spray in the environment or combustion chamber (Lefebvre, 1989).

In general, large angles (greater than 100º) promoting the atomization of the liquid by print to spray a large tangential velocity component. But the spray cone angle cannot be so large, in order to avoid the fuel spraying on the wall leading to the coke. Small angles (smaller than 60°) promoting the penetration of spray into the environment due to the higher axial velocity component. However, they tend to displace the combustion zone away from the injector and can result in problems of combustion stability. Furthermore, if the spray cone angle is too small, the fuel will be sprayed into the recirculation zone less oxygen and then causes much more pyrolysis.

The spray cone angle is measured from digital photographs for each pre-defined condition. The photos are inserted into a treatment program image where two straight lines are drawn at the exit orifice tangent to the spray, allowing to measure the angle of the spray.

2.3 Discharge coefficient

The discharge coefficient is an important parameter in designer of the injector, and it directly decides the success or failure of the design. If the discharge coefficient is much big, the outlet area will be much bigger than the necessary, so as to influence the spray quality of the injector. If the discharge coefficient is small, the designed mass flow rate cannot be achieved and consequently cannot satisfy the need of the temperature and flame length.

Considering incompressible flow, adiabatic flow, no variation of gravitational potential energy, the discharge coefficient of the liquid is obtained from the continuity equation (Delmeé, 1983):

$$c_{d,l} = \frac{\dot{m}_l}{A\sqrt{2\rho_l \Delta P_l}} \tag{2}$$

where $c_{d,l}$ is the discharge coefficient of the liquid; $\dot{m}_l$ the liquid mass flow rate, kg/s; A the total cross-sectional area of the discharge orifices, m^2; ρ_l the density of the liquid, kg/m^3; $\Delta P_l = P_{l,inj} - P_{amb}$ the pressure difference of the liquid flow across the injector, Pa (P_{amb} is the ambient pressure and $P_{l,inj}$ is the liquid injection pressure).

To determine the discharge coefficient, the liquid is collected in a graduated recipient during 10 s and after the liquid mass in the recipient is measured and the average mass flow rate in this period is calculated. So the discharge coefficient of liquid and air can be obtained from Eq. (2).

3. RESULTS AND DISCUTION

In this section are shown the results obtained in the characterization of the blurry injector for the case where H = 0.125 mm.

3.1 Pressure Measurements

The injection pressure was measured by a pressure transducer (0–20 bar range) installed upstream of the atomizer using a T-junction. The measured pressure was effectively the pressure drop in the line because the atomizer was open to the ambient. The typical curve of the mass flow rates for liquid and air changed with injection pressure is shown in Fig. 4.

It can be shown from the figure that the mass flow rates of the liquid and air increase with the pressure increasing and the air increases faster than the liquid because the compressibility of the air is bigger than that of the liquids. With increasing of the pressure, the trend will be obvious more and more. Furthermore, the liquid flow rate is seen to increase with an increase in liquid injection pressure, which is expected due to the increase in incoming liquid velocity with the increase in injection pressure. It is observed that the mass flow rate of water is higher that the mass flow of B 100 soy biodiesel and hydrous ethanol.

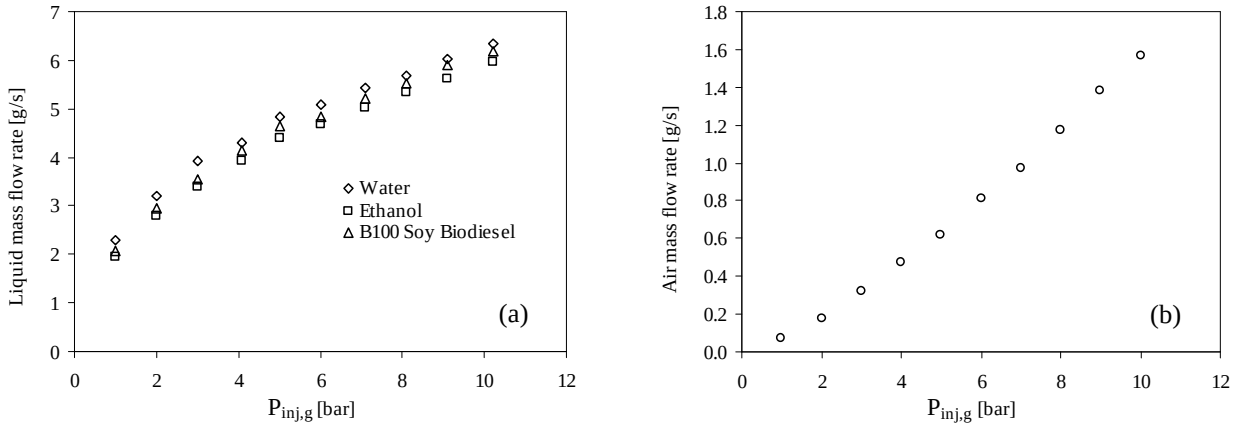

Figure 4. Curve of the mass flow rates versus injection pressure: (a) liquid mass flow without atomizing air flow; (b) air mass flow rate without liquid flow.

In the present study, the liquid injection pressure was initially kept constant and the air flow rate was varied over a range by changing the air injection pressure to obtain the variation in Air to Liquid Mass Ratio (ALR). The liquid injection pressure was then varied and the entire procedure was repeated for different values of air injection pressure. The spray characteristics corresponding to a range of liquid injection pressures, air injection pressure and Air to Liquid Mass Ratio (ALR) were studied and the results are presented in the next section.

The full operating envelop reported in this paper is given in Fig. 5.

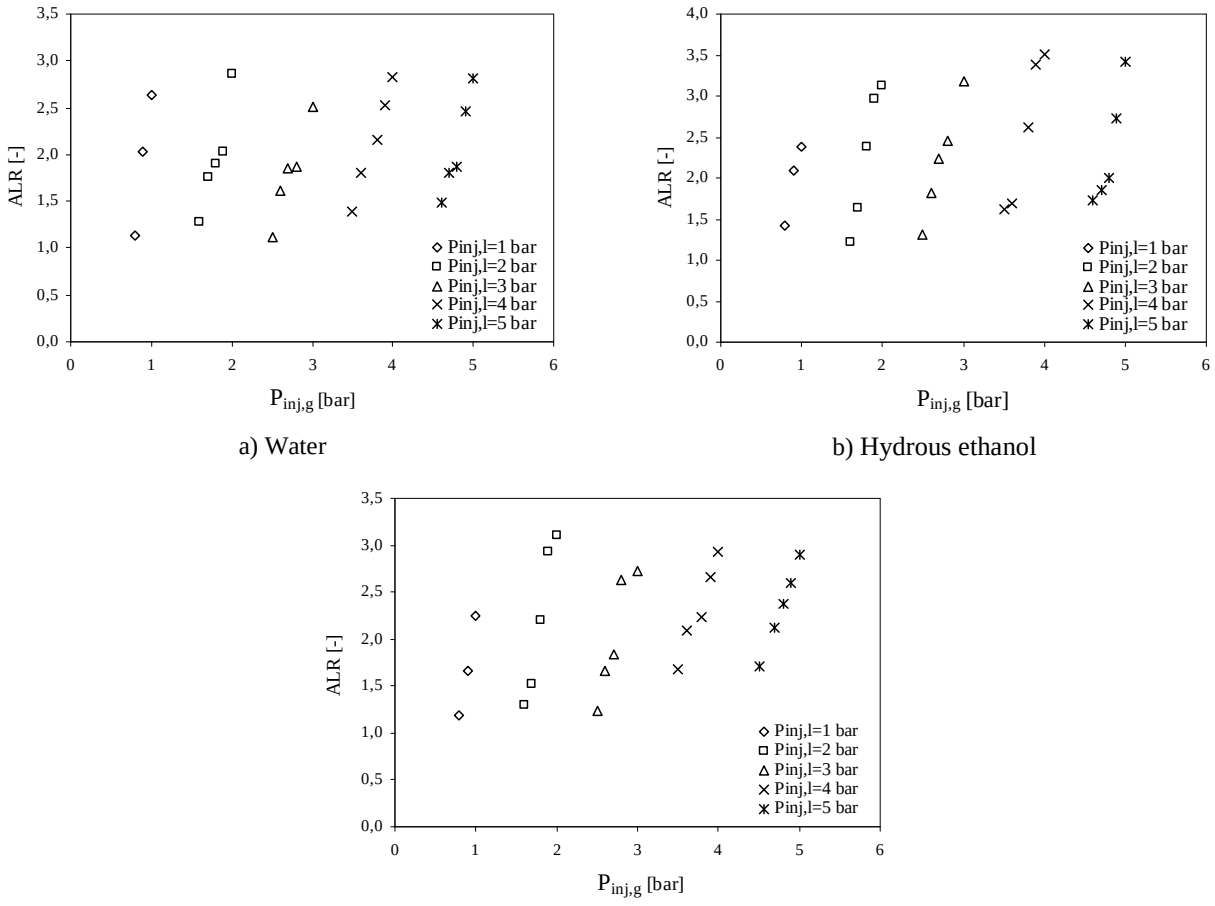

a) Water

b) Hydrous ethanol

c) B100 soy biodiesel

Figure 5. Full operating envelop of the blurry injector.

It is observed that for a given liquid injection pressure an increase in the air injection pressure leads to an increase in ALR, once an increase in air injection pressure causes an increase in air mass flow rate and the liquid mass flow rate is kept constant.

The variation of liquid and air flow rate with ALR for different liquid injection pressures is shown in Fig. 6

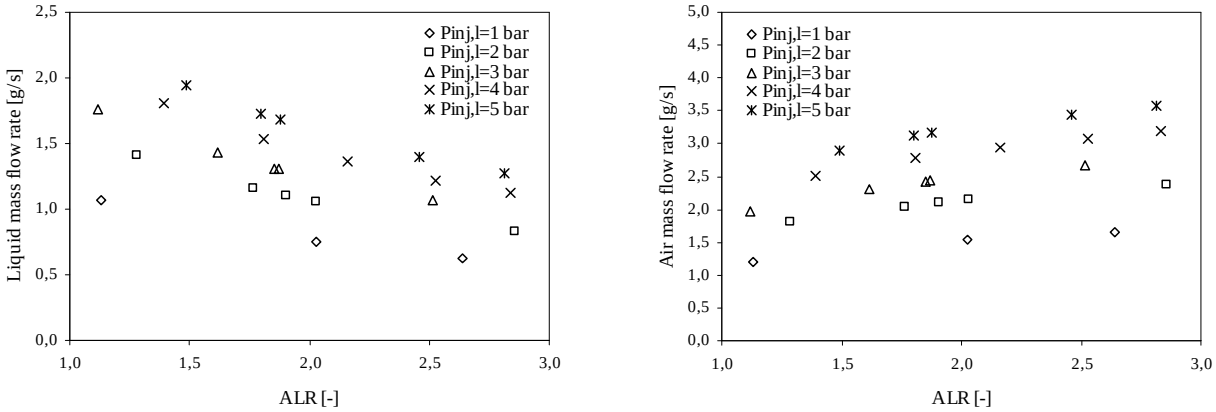

a) Water

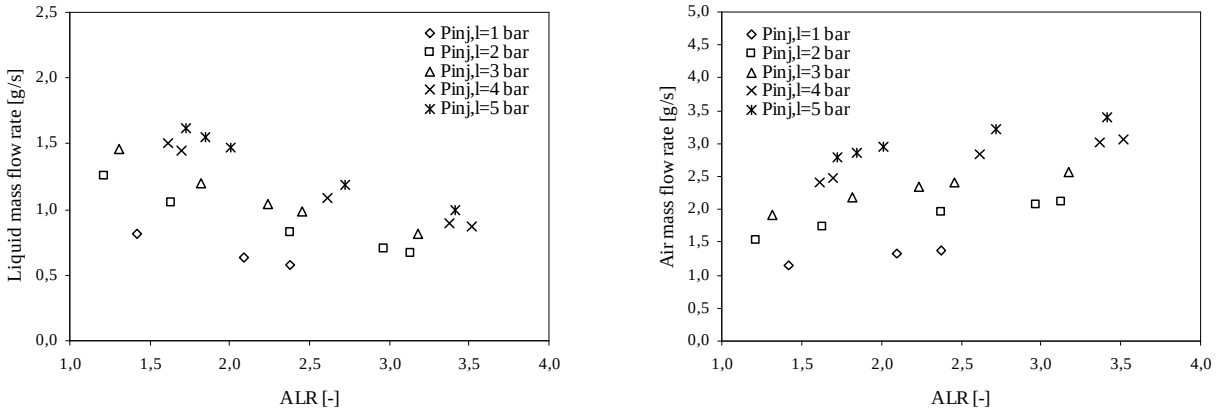

b) Hydrous ethanol

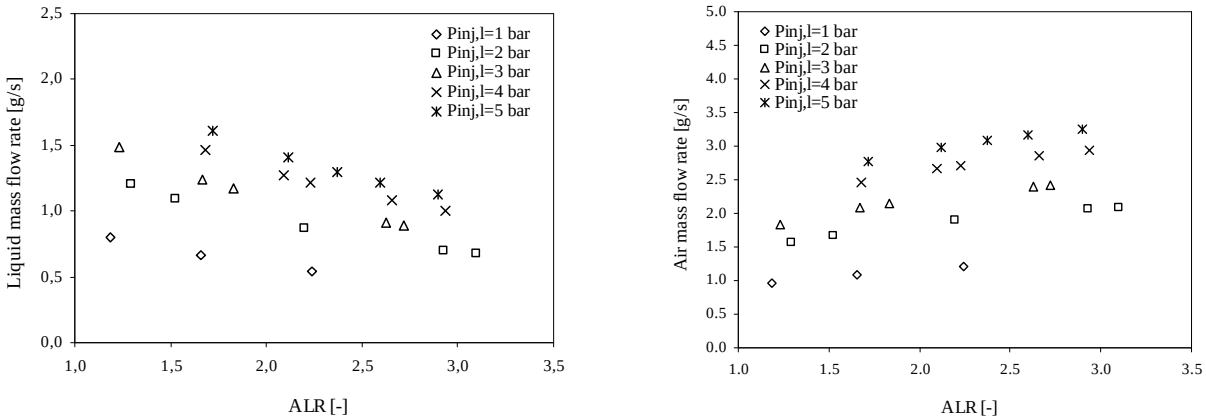

c) B100 soy biodiesel

Figure 6. Variation of liquid and air flow rate with ALR for different liquid injection pressures.

The data presented in this figures shown that the liquid mass flow rate decreases with an increase in ALR. At lower values of ALR the decrease is quite rapid. But, at higher values of ALR, the change in liquid mass flow rate is quite small with an increase in ALR for a particular liquid injection pressure. Furthermore, the liquid mass flow rate is seen to increase with an increase in liquid injection pressure, which is expected due to the increase in incoming liquid velocity with the increase in injection pressure. It is observed that the air mass flow rate increases with an increase in ALR, once

an increase in the air injection pressure causes an increase in incoming air velocity and consequently an increase in the air mass flow rate. It is observed that an increase in the liquid injection pressure leads to an increase in the air mass flow rate, once a larger amount of air is necessary to obtain the spray.

3.2 Spray cone angle

Figures 7, 8 and 9 shown a collection of spray images obtained from the high-speed photography for the water, hydrous ethanol and B100 soy biodiesel.

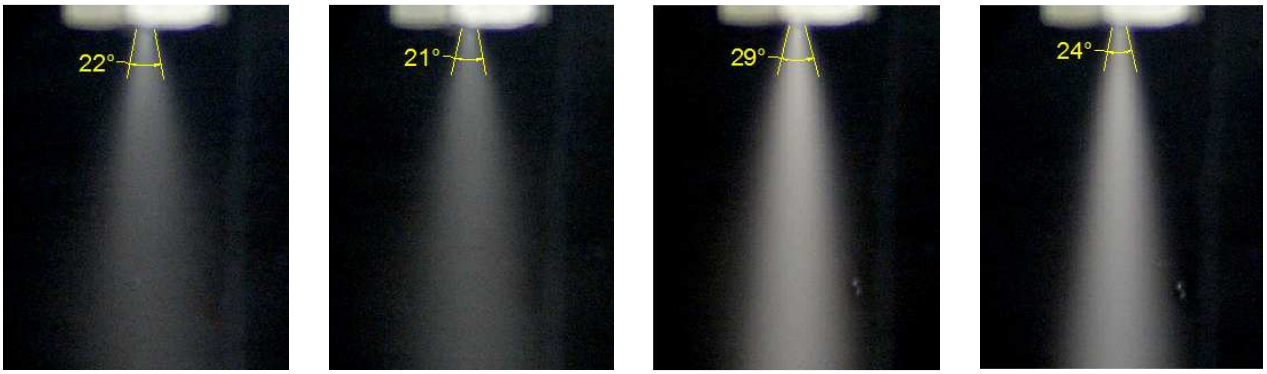

a) $\Delta P_l = 1$ and $\Delta P_g = 0.8$ bar b) $\Delta P_l = 1$and $\Delta P_g = 0.9$ bar c) $\Delta P_l = 5$and $\Delta P_g = 4.8$ bar d) $\Delta P_l = 5$ and $\Delta P_g = 4.9$ bar

Figure 7. Spray cone angle for the blurry injector using water.

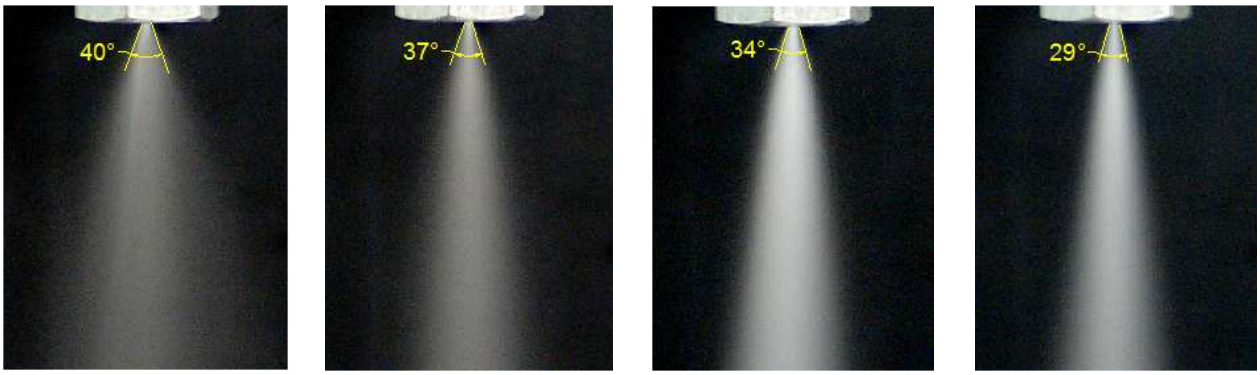

a) $\Delta P_l = 1$ and $\Delta P_g = 0.8$ bar b) $\Delta P_l = 1$and $\Delta P_g = 0.9$ bar c) $\Delta P_l = 5$and $\Delta P_g = 4.8$ bar d) $\Delta P_l = 5$and $\Delta P_g = 4.9$ bar

Figure 8. Spray cone angle for the blurry injector using hydrous ethanol.

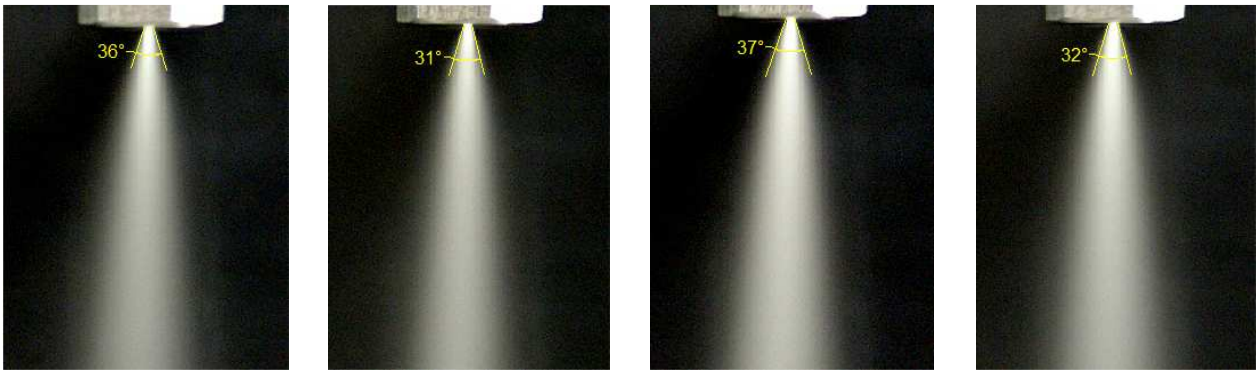

a) $\Delta P_l = 1$ and $\Delta P_g = 0.8$ bar b) $\Delta P_l = 1$and $\Delta P_g = 0.9$ bar c) $\Delta P_l = 5$and $\Delta P_g = 4.8$ bar d) $\Delta P_l = 5$and $\Delta P_g = 4.9$ bar

Figure 9. Spray cone angle for the blurry injector using B100 soy biodiesel.

Figures 7, 8 and 9 are the spray photographs for the blurry injector with different pressures. It is observed from the photographs that with the increasing of the air pressure, the atomization is improved obviously. For a fixed liquid pressure an increase in the air pressure, thus increasing the ALR, it is observed that the spray cone angle decreases. It is observed that for low pressures the bigger cone angles are obtained to the hydrous ethanol while for high pressures the bigger angles are obtained for the B100 soy biodiesel.

3.3 Sauter Mean Diameter

The dependence of droplet Sauter Mean Diameter (SMD) and Mass Median Diameter on Air Liquid Mass Ratio (ALR) for different liquid injection pressure are shown in Figs 10, 11 and 12.

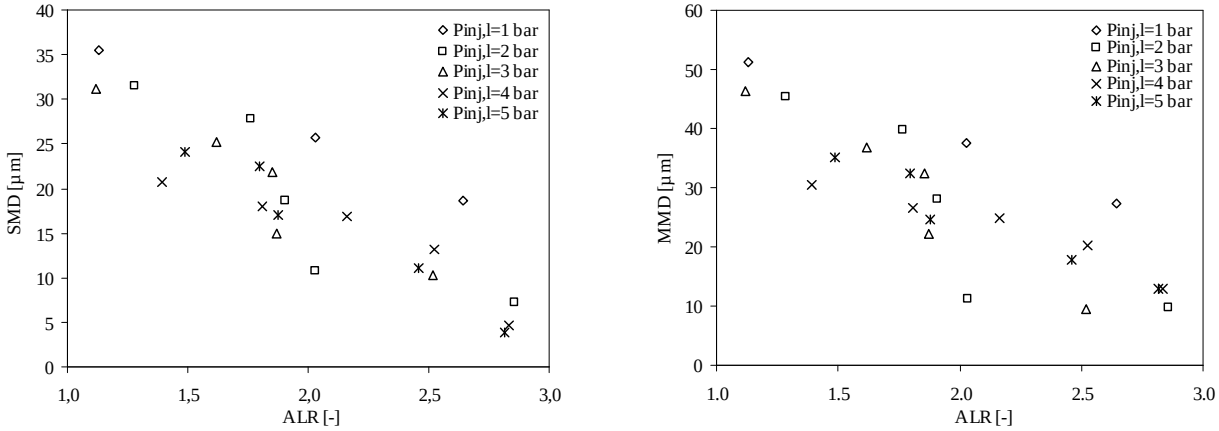

Figure 10. Experimental Sauter mean diameter (SMD) and mass median diameter (MMD) for water.

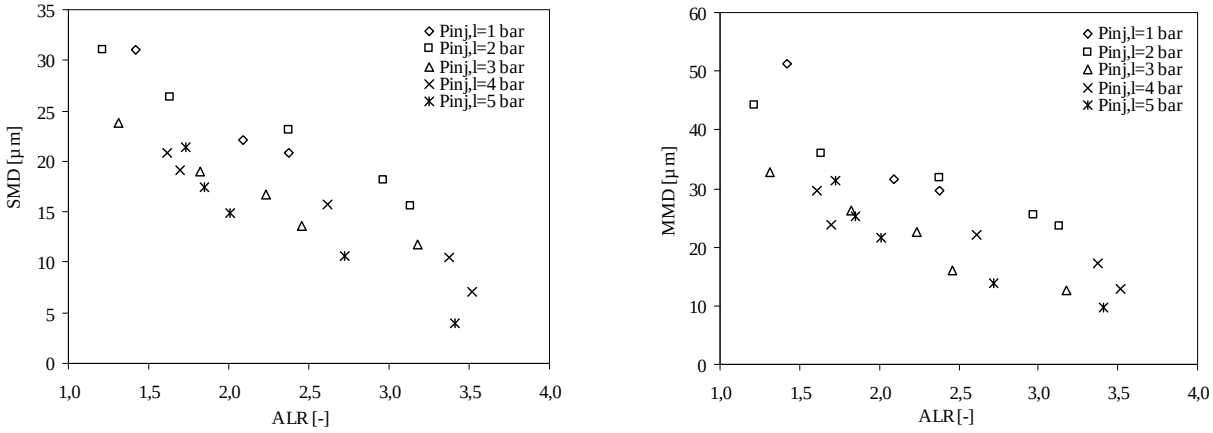

Figure 11. Experimental Sauter mean diameter (SMD) and mass median diameter (MMD) for hydrous ethanol.

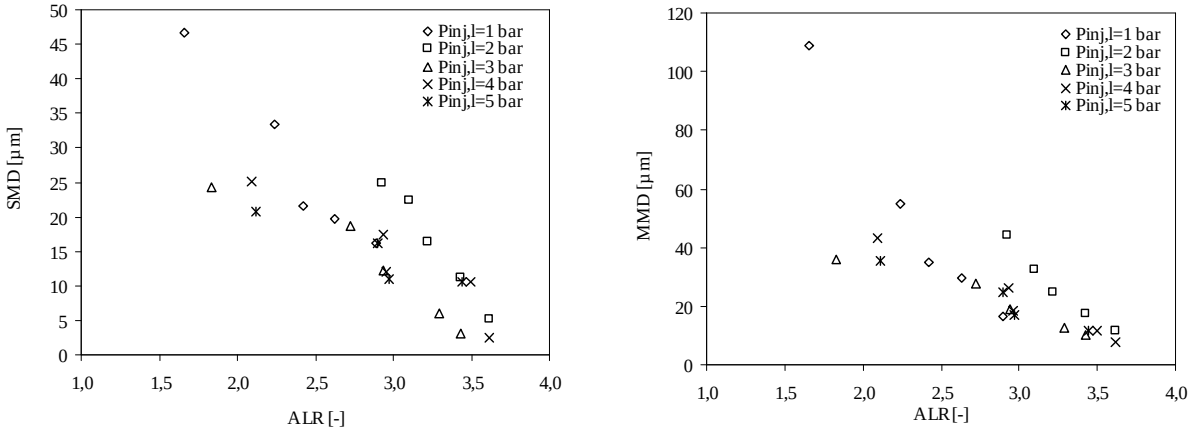

Figure 12. Experimental Sauter mean diameter (SMD) and mass median diameter (MMD) for B100 soy biodiesel.

The data presented in Figs 10, 11 and 12 shown that the droplet size decreases with an increase in ALR for a given liquid injection pressure. It can be seen in Figs 10, 11 and 12 that the droplet size decreases in general with an increase in liquid injection pressure. This can be attributed to the increase in liquid kinetic energy and, hence, in inertial forces

acting on the liquid with an increase in its injection pressure, resulting in finer atomization. However, for a given liquid injection pressure, there is a rapid decrease in droplet SMD at lower values of ALR.

As expected, it is observed that an increase in the liquid injection pressure leads to decrease in MMD, and an increase in ARL causes a decrease in MMD.

The data presented in Fig. 10 shows that SMD for water varies between 35.48 μm to 3.889 μm and MMD decreases 51.16 μm to 13.01 μm over the entire operating range. For the hydrous ethanol, the data presented in Fig. 11 shows that SMD varies between 30.98 μm to 3.987 μm and MMD decreases from 51.19 μm to 9.60 μm over the entire operating range. The data presented in Fig. 12 shows that SMD for B100 soy biodiesel varies between 46.75 μm to 2.30 μm and MMD decreases 108.9 μm to 7.48 μm over the entire operating range. For the same conditions it is verified that the larger droplets are obtained when the working fluid is B100 soy biodiesel and the smaller droplets are obtained when the working fluid is the hydrous ethanol.

3.5 Discharge coefficient

Figure 13 shows the typical curve of the discharge coefficient versus ALR.

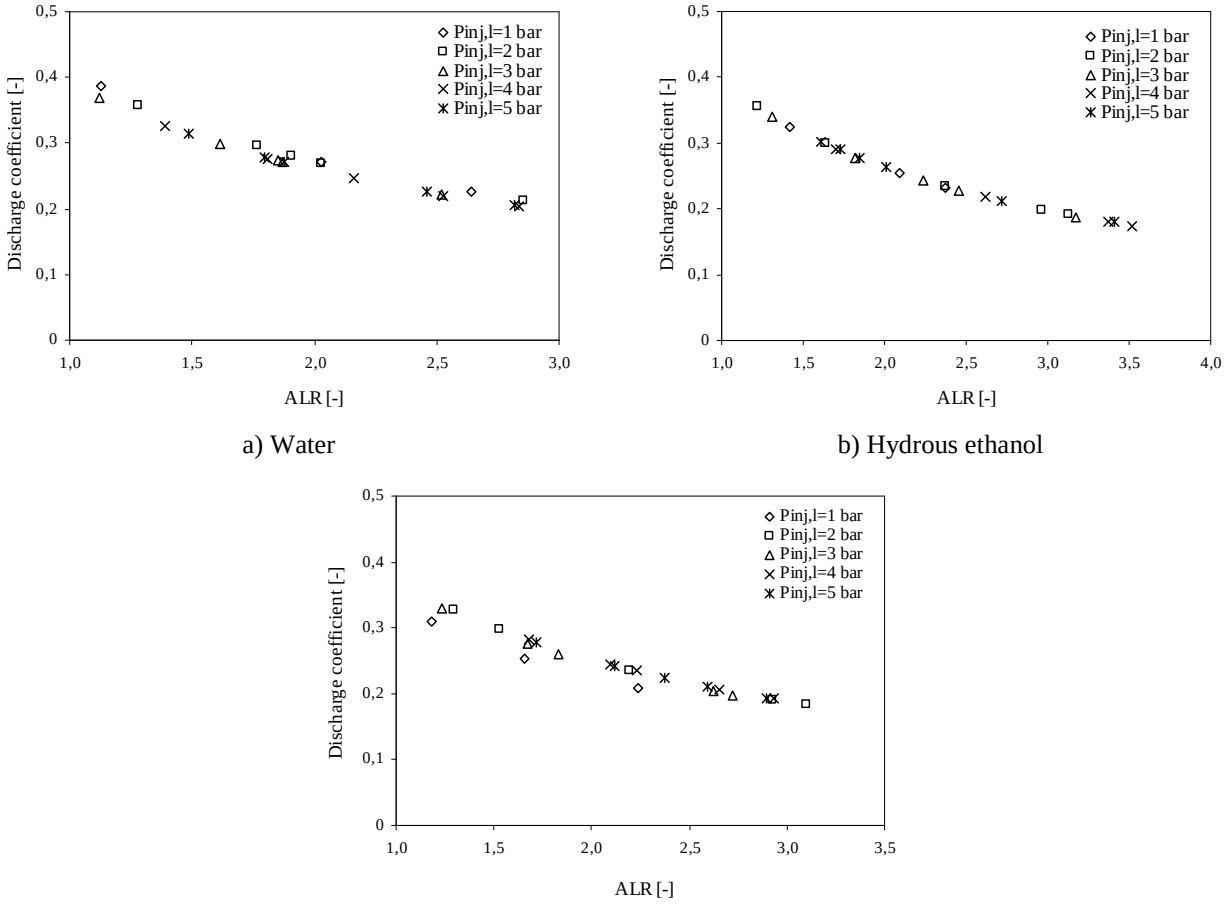

a) Water

b) Hydrous ethanol

c) B100 soy biodiesel

Figure 9. Typical curve of the discharge coefficient versus ALR.

The data presented in Fig. 13 shows that the discharge coefficient decreases with an increase in ALR. Lefebvre, 1983 has defined the discharge coefficient to be a measure of the extent to which the liquid flowing through the final discharge orifice makes full use of the available flow area. Therefore, the reduction in discharge coefficient with ALR points to the fact that the flow area available for liquid decrease with an increase in ALR, and, the reduction in liquid flow rate with an increase in ALR can be safely attributed to the reduction in flow area of the liquid. The rate of change of $c_{d,l}$ with ALR is inversely proportional to ALR. Therefore, the rate of change decreases with an increase in ALR, which is responsible for slower rate of decrease in the liquid flow rate at higher values of ALR. This behavior may be attributed to the change in two-phase flow regime with ALR.

4. CONCLUSIONS

Spray characteristics of a blurry injector using water, hydrous ethanol and B100 soy biodiesel as the test fluids are presented.

From experiments it is verified that the flow blurring regime occurs only for a certain range of liquid and air pressure. If the liquid pressure is greater than the air pressure, occurs the formation of a capillary jet, and if the air pressure is greater than liquid pressure, air blocks the flow of liquid. Thus, there is an optimum pressure of liquid and air to work with the blurry injector.

The liquid flow rate is seen to decrease with an increase in air liquid mass ratio, which is attributed to a decrease in available area for liquid flow with increasing air flow rate. The droplet diameter is seen to decrease with an increase in air liquid mass ratio and liquid injection pressure due to an increase in inertial forces.

5. ACKNOWLEDGEMENTS

The authors acknowledge Vale Energy Solutions for providing a scholarship.

6. REFERENCES

Delmeé G. J,. 1983, “Manual de Medição de Vazão”, São Paulo: Editora Edgard Blucher. 474p.

Gañán-Calvo, A. M., 1998, “Generation of Steady Liquid Microthreads and Micro-Sized Monodisperse Sprays in Gas Streams”, Physical Review Letters, Vol.80, Nº2, pp. 285-288.

Gañán-Calvo, A. M., Barrero, A. 1999, “A Novel Pneumatic Technique to Generate Steady Capillary Microjets”, J. Aerosol Sci., Vol.30, pp. 117-125.

Gañán-Calvo, A. M., 2005, “Enhanced Liquid Atomization: From Flow-Focusing to Flow-Blurring”, Applied Physics Letters 86.

Gong, J.S., Fu, W.B., 2007, “The experimental study on the flow characteristics for a swirling gas–liquid spray atomizer”, Applied Thermal Engineering, Vol. 27, pp. 2886–2892.

Lefebvre, A.H., 1983, “Gas Turbine Combustion”, Hemisphere, Washington, D.C.

Lefebvre, A.H., 1989, “Atomization and Sprays”, Hemisphere, New York.

Panchasara, H. V., Sequera, D. E., Schreiber, W. C., Agrawal, A. K., 2009, “Emissions Reductions in Diesel and Kerosene Flames Using a Novel Fuel Injector”, Journal of Propulsion and Power. Vol. 25, No. 4.

Sadasivuni, V., Agrawal, A. K., 2009, “A novel meso-scale Combustion System for Operation with Liquid Fuels”, Proceedings of the Combustion Institute, 32, pp. 3155–3162.

Simmons, B., Agrawal, A. K., 2010, “Spray Characterization of a Flow-Blurring Atomizer”, Atomization and Sprays, Vol 20, pp. 821–835.

Wünning, J. A., Wünning, J. G., 1997, “Flameless Oxidation to Reduce Thermal No-formation”, Progress in Energy and Combustion Science, 23, Issue 1, 1997, pp.81-94.

7. RESPONSIBILITY NOTICE

The authors are the only responsible for the printed material included in this paper.